www.nts.com
1.800.270.2516

Methodology for Transient Thermal Analysis of Machine Gun Barrels Subjected to Burst Firing Schedules

Authors: Ryan Hill and Logan McLeod

This work presents a method for simulating the heating of machine gun barrels during burst firings. The method utilizes a two-dimensional axisymmetric finite element model which solves the highly transient convection input on the bore wall, conduction through the barrel, and convective and radiative cooling on the outside wall. The transient input is derived from a coupling of a lumped-parameter interior ballistics code with a one-dimensional compressible flow model which includes the discharge of the combustion product gas behind the projectile. This transient convective boundary condition can be repeated as desired for arbitrary firing schedules. Finally, an example simulation is performed on a small caliber machine gun and compared with experimental data.

Introduction

For reasons such as performance, cost, and weight, small arms ammunition is under constant development and improvement. For example, there has been long-standing interest in the development of cartridges employing new, higher energy propellants, and machine gun barrels fabricated using new processes and innovative heat resistant materials. One challenge associated with fielding new ammunition or incorporating new materials into an existing gun system is predicting how the modifications may affect the performance, operation, longevity, and safety of the weapon. From a thermal perspective, there are three issues of relevance: 1. the magnitude and spatial distribution of the heat load on the bore wall which is closely linked to erosion and barrel longevity, 2. the total heat input to the barrel over extended burst firing schedules which may affect accuracy, and 3. the amount of heat which may be conducted back into the breech and lead to a cook-off event or cause other thermal degradation of a chambered round. Understanding the role these issues may play in a modified weapon requires the ability to model the extended burst firing schedules that the weapon may see during qualification and, ultimately, combat.

The true physical and chemical processes which occur during the firing of a single round from a small arms weapon are highly complex; from pressure-dependent chemical kinetics of propellant combustion to compressible fluid dynamics and turbulent boundary layer development. Modeling all of these processes in order to accurately predict the interaction of a single round with the gun barrel assembly is a difficult task. Attempting to extend this model in order to predict the effects of extended burst firings with various burst schedules quickly becomes computationally intractable.

In this work, a simplified model is developed which couples a lumped-parameter interior ballistics calculation with a finite element thermal model of the barrel assembly geometry. The interior ballistics model permits calculation of the combustion product gas properties as functions of time and barrel axial position for a single round and can account for complexities such as variations in propellant load, burn rate, shot start pressure, etc. The bulk gas property predictions from the interior ballistics model are then used in combination with a standard convective heat transfer correlation to calculate the heat transfer coefficient and gas temperature for a single bullet, both functions of time and axial position. Finally, the heat transfer coefficient and gas temperature can be repeated to simulate any arbitrary burst firing schedule and then applied to the finite element thermal model as a convective heat transfer boundary condition. This model is an improvement upon the recent work of [1] with an enhanced treatment of the venting of the combustion product gas following the projectile exit.

This manuscript will present the details of the modeling approach, and model implementation will be demonstrated. Modeling predictions for the bore wall temperature as well as the barrel outer surface will be compared with test data available in the public domain taken from extended burst firing of the M80 cartridge from the M60 machine gun.

Model Development

The simplified model developed in this work can be divided into two distinct parts. The first part involves the calculation of the convective heat transfer coefficient at the bore wall h and the gas temperature in the gun bore T_g using a combination of interior ballistics and a one dimensional compressible flow model. These two quantities will be used to calculate the instantaneous local heat flux q'' on the bore wall using equation (1), where T_s is the local bore surface temperature.

$$q'' = h\left(T_g - T_s\right) \tag{1}$$

The second part solves the transient conduction problem in the gun barrel assembly subject to the bore wall boundary condition developed in step one as well as appropriate boundary conditions on the other domain boundaries.

When a round is fired, the heat transfer coefficient and bore gas temperature will both be continuous functions of time and axial position. However, in order to apply this boundary condition to the model the bore surface must be divided into a finite number of regions. The values of h and T_g, now only functions of time, are calculated at the center of each bore surface region and the boundary condition is enforced uniformly over the entire region. Depending on the spatial resolution desired from the model these regions can be as small as a single element on the discretized surface or as large as the entire length of the barrel.

Part One – Determination of Bore Wall Boundary Conditions

Calculation of the bore wall heat transfer coefficient and free-stream gas temperature for an entire simulated burst firing is, in itself, a multi-step process. The first step is to develop an accurate interior ballistics model for the ammunition item and barrel of interest. This work utilizes a modified Baer-Frankle [2] interior ballistics code in Arrow Tech Associates' PRODAS software [3]. The Baer-Frankle code is a lumped-parameter model which simulates the combustion process based on the properties of a propellant, such as flame temperature, impetus, burn rates, grain geometry, covolume, ratio of specific heats, etc. This model can be tuned either by collecting burn rate data directly from propellant characterization tests or by adjusting the burn rate properties to match experimentally measured gun fire data, such as maximum breech pressure and muzzle velocity. The results of the lumped-parameter Baer-Frankle simulation are then used to create a one-dimensional compressible flow model which calculates the combustion gas density ρ, velocity v, and temperature T_g at any axial position for the complete firing cycle.

Armed with the thermodynamic and flow conditions of the reaction product gas, the heat transfer coefficient can be calculated from a convective heat transfer correlation for fully developed turbulent pipe flow, which expresses the Nusselt number Nu as a function of the Reynolds and Prandtl numbers Re and Pr [4]

$$Nu = 0.023\, Re^{0.8}\, Pr^{0.3}\, K_e \tag{2}$$

with the addition of a nondimensional entrance factor K_e [5]. Since the original correlation in [4] is for a fully developed flow, K_e is a function of axial position which accounts for the fact that the flow is not fully developed in the breech. Its value is approximately 1.75 at the breech and it decays to 1 at a distance of roughly 40 calibers, where the flow is thought to be fully developed.

For flow in a pipe of circular cross section of diameter D, if the gas has a velocity v, density ρ, viscosity μ, and thermal conductivity k, the definitions of the Nusselt and Reynolds numbers are, respectively:

$$Nu = \frac{h\,D}{k}, \quad Re = \frac{\rho\, v\, D}{\mu} \tag{3}$$

Comparing equations (2) and (3), it is possible to solve for h:

$$h = 0.023\,\frac{k}{D}\left(\frac{\rho\, v\, D}{\mu}\right)^{0.8} Pr^{0.3}\, K_e \tag{4}$$

where k and μ are functions of temperature, computed using the Lennard-Jones potential technique of [6] and the assumed combustion products of a nitrocellulose-nitroglycerin double-base propellant as in [7]. A suitable value for Pr is 0.75 according to [5]. It remains to calculate the combustion gas properties T_g, ρ and v as functions of time and axial position for the firing cycle.

Calculation of Gas Properties

The output of the initial Baer-Frankle analysis includes the projectile base position z_p, projectile velocity v_p, volume V, fraction of propellant burnt F, and average gas temperature T_{avg} as functions of time t.

The total firing cycle is broken into four time segments: 1. while the projectile is in the barrel, 2. after projectile exit while a rarefaction wave travels backward down the barrel, 3. after the rarefaction wave reaches the breech, and 4. where there is no more heat transfer in the bore.

In order to simplify the equations, the axial position z is scaled by the projectile base position z_p to obtain a nondimensional normalized axial coordinate:

$$\xi = \frac{z}{z_p} \tag{5}$$

First Time Segment

While the projectile is still in the barrel, it is assumed that the velocity v of the gas is linear from zero at the breech to v_p at z_p:

$$v = v_p \, \xi \tag{6}$$

and the thermodynamic state variables density ρ, temperature T_g, and pressure P are determined by the equations:

$$\frac{1}{\rho} - \eta = \left(\frac{V}{C F} - \eta \right) \left(1 + \frac{C F}{6 \gamma W} \left(3 \xi^2 - 1 \right) \right) \tag{7}$$

$$T_g = T_{avg} \left(1 + \left(\gamma - 1 \right) \frac{C F}{6 \gamma W} \left(1 - 3 \xi^2 \right) \right) \tag{8}$$

$$P = R T_{avg} \left(\frac{V}{C F} - \eta \right)^{\gamma - 1} \left(\frac{1}{\rho} - \eta \right)^{-\gamma} \tag{9}$$

where C is the propellant charge weight, W is the projectile weight, and R, η and γ are respectively the specific gas constant, covolume and ratio of specific heats of the combustion product gas.

With the exception that the current definition of ξ differs from that in [8], when the projectile reaches the muzzle and the propellant is all burnt, equations (6) through (9) are equivalent to the initial conditions in [8], which is used as the basis for the second segment.

Second Time Segment

The second segment of the problem begins with the bullet just out of the muzzle and the gas in the state described in equations (6) through (9). Note that after the muzzle exit, equation (9) is evaluated using $T_{avg} = T_m$, the average temperature at the time of muzzle exit, $V = V_m$, the total internal volume of the gun, and $F = 1$, since the propellant is burned out before the projectile reaches the muzzle. The speed of sound c in the gas is, using equation (9):

$$c = \left(\frac{dP}{d\rho} \right)^{1/2} = \frac{\left(\gamma R T_m \right)^{1/2}}{1 - \eta \rho} \left(\frac{V_m}{C} - \eta \right)^{\frac{\gamma - 1}{2}} \left(\frac{1}{\rho} - \eta \right)^{\frac{1 - \gamma}{2}} \tag{10}$$

Because c is greater than the projectile muzzle velocity v_m for this cartridge, a rarefaction wave immediately begins at the muzzle and flows toward the breech at the time of muzzle exit t_m. The solution for the second segment comes from [8], but with a few slight modifications.

After the projectile leaves the muzzle, z_p is replaced with the barrel length L in calculating ξ. For consistency, a nondimensional time τ is defined in such a way that $\partial \xi / \partial \tau$ is equivalent to that in [8], even though the nondimensional coordinates themselves are defined differently in this present work:

$$\xi = \frac{z}{L}, \quad \tau = \frac{v_m}{L} \left(t - t_m \right) \tag{11}$$

Another difference in this model is that once the rarefaction wave passes a given point, the velocity profile is assumed to be linear with respect to ξ between that point and the muzzle. The endpoints of this linear region are calculated such that the velocity is continuous at the position of the rarefaction wave and that $v = c$ at the muzzle (due to a choked flow condition).

Once the gas velocity and density are determined, the pressure is calculated using equation (9) with $F = 1$, $V = V_m$ and $T_{avg} = T_m$. Let T_0 and P_0 be the temperature and pressure at the breech at the time of muzzle exit ($\xi = 0$, $\tau = 0$). Since there is no more propellant burning and the time scale is short, the assumption is made that the temperature and pressure of the gas lie on the same adiabat for all $\tau \geq 0$. Since the PRODAS output ends at $\tau = 0$, T_{avg} is no longer given as a function of time, so in this segment the temperature is calculated by the relation:

$$\frac{T_g}{T_0} = \left(\frac{P}{P_0}\right)^{\frac{\gamma-1}{\gamma}} \tag{12}$$

Third Time Segment

For simplicity this work does not consider the reflection of the rarefaction wave off of the breech face; the wave is ignored after this point. At this time the problem described in [8] is complete. What remains is a velocity profile which varies from c at the muzzle to zero at the breech and a density profile, which is also linear with respect to ξ.

In order to further exhaust the gas from the barrel in the third segment, it is assumed that the density profile remains linear in ξ and decays exponentially with time. The decay rate is constant in ξ and is chosen so that $\partial\rho/\partial\tau$ is continuous at the muzzle ($\xi = 1$) at the time the rarefaction wave reaches the breech.

The linear velocity distribution is also maintained from ($v = 0$, $\xi = 0$) to ($v = c$, $\xi = 1$). It is noted however, that since c is proportional to density, c at the muzzle will decrease in time, and in turn so does the velocity.

Since the expansion of the gas is still rapid, the gas pressure and temperature continue along the same adiabat from the second segment, and they are also calculated here using equation (9) with $F = 1$, $V = V_m$ and $T_{avg} = T_m$ and equation (12).

For these first three time segments, the gas density and velocity are used as inputs to the finite element model. In fact, these three segments compose the entire heat input, since $h = 0$ in the fourth segment.

Fourth Time Segment

The combination of a high gas density and a short time scale allows for the adiabatic assumptions used in the second and third time segments. However, at some point, the gas density becomes small enough that heat transfer between the gas and the bore wall will cause appreciable temperature change in the gas. This would result in thermal equilibration between the gas and the bore wall with no subsequent heat transfer occurring. Since the gas temperature is specified *a priori* with no knowledge of the resulting bore-wall temperature, h is forced to zero once the gas pressure at the muzzle drops below 10 atm, which typically occurs after a few milliseconds for small caliber rifles. The use of 10 atm as a threshold is somewhat arbitrary, but the vast majority of the heat input has been captured by this time. It is this condition that marks the beginning of the fourth time segment, in which there is no heat transfer at the inside wall of the barrel until the subsequent round is fired.

Repeating Boundary Condition

The final step in Part One is to repeat the boundary condition described in the four time segments above. One simplification to the problem is the assumption that the interior ballistics cycle is independent of the starting barrel temperature, and thus the gas temperature, velocity and density are identical for each round [9]. With this assumption, the boundary condition at the bore wall can be repeated for an arbitrary firing rate and burst schedule. As in the fourth time segment, there is no heat transfer at the bore wall for long intervals between bursts.

Part Two – Transient Heat Conduction in the Gun Barrel

Having calculated the bore wall boundary condition, the second part of the model can be implemented. This involves solving the heat conduction equation (13) over the domain of interest, namely the barrel assembly

$$\frac{\partial T}{\partial t} = \alpha \nabla^2 T \tag{13}$$

where T is the temperature and α is the thermal diffusivity for the material under consideration.

The heat equation can be discretized in the calculation domain using a variety of techniques, the most common being the finite difference, the finite volume, and the finite element methods. In this work the spatial computational domain is discretized using the finite element method while the time domain is discretized using a backward difference method, resulting in an implicit transient calculation.

As previously mentioned, the bore wall is subdivided into distinct regions for application of the convective boundary condition. The center of each region is coincident with an axial calculation location output from the interior ballistics analysis of Part One. The time-dependent heat transfer coefficient and gas temperature are utilized to calculate the instantaneous local heat flux using equation (1), which is enforced as a boundary condition along each region of the bore wall. As can be seen in equation (1), although the gas temperature and heat transfer coefficient are fully specified before starting the simulation in Part Two, the heat flux at a specific time and location on the bore wall depend on the instantaneous local

surface temperature T_s. Therefore the heat flux into the barrel varies for each round due to the fact that the temperature profile along the bore wall is different at the time each round is fired.

After the last round in a burst is fired, the bore wall is assumed to have an adiabatic boundary condition Due to the small thermal mass of the gas in the bore, it will quickly equilibrate with the bore wall and further heat transfer will be negligible. Near the muzzle gas exchange will cause accelerated cooling; this complexity is neglected.

The boundary condition on the outer surface of the barrel is modeled with a combination of convection and radiation heat transfer. The main factors affecting the convective heat transfer coefficient are the barrel outer diameter and the ambient wind conditions. Considering wind conditions ranging from stagnant (natural convection only) up to 10 meters per second, and the range of barrel outer diameters applicable to small arms yields a convective heat transfer coefficient which ranges from 5 to 90 W/m^2-K. While this variation is quite large, the actual rate of heat transfer from the outer surface of the barrel is extremely small relative to the heat input on the bore wall. During burst firing, the barrel temperature rises quickly and will equilibrate in the radial direction before any significant amount of heat is lost to the surrounding environment; therefore the peak temperatures observed on the outer surface of the barrel are relatively insensitive to the value of heat transfer coefficient utilized. However, the long duration cooling rate of the barrel does depend strongly on the heat transfer coefficient. The barrel outer surface is assumed to have an emissivity value of 0.95 for calculation of the radiative heat transfer into the ambient surroundings.

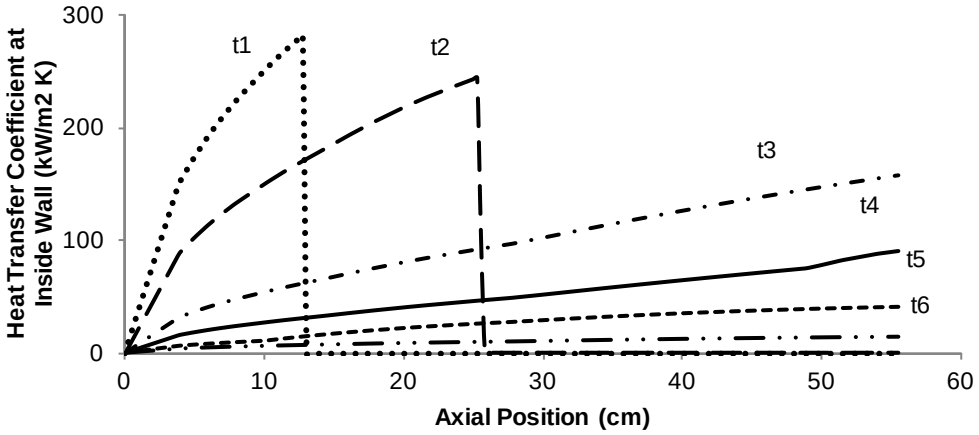

Figure 1. Interior wall heat transfer coefficient vs. axial position for various times in the firing cycle.

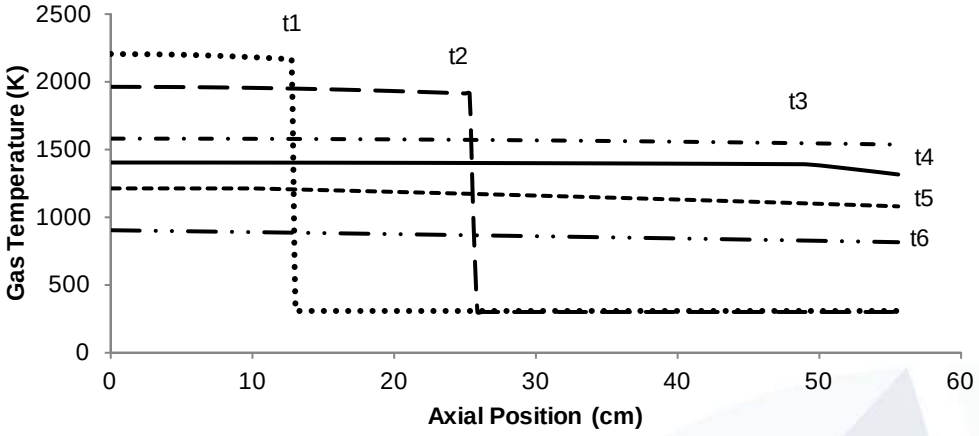

Figure 2. Bore gas temperature vs. axial position for various times in the firing cycle.

Model Validation

Experimental data for the 7.62-mm M80 ball cartridge as fired from the M60 machine gun are available in the public domain [12]. The interior ballistics analysis and implementation of the finite element model for this weapon are presented below, along with a comparison of the modeling results with the experimental data.

Heat Input as Function of Time and Axial Position

Time evolutions of the axial distributions for the heat transfer coefficient at the bore wall and the gas temperature as calculated in Part One above are plotted in Figures 1 and 2. The first two curves in each figure show the distributions while the projectile is still in the barrel. The projectile has traveled a distance of 13 cm at t1 (0.54 ms) and 26 cm at t2 (0.75 ms). The vertical line in each curve at these two axial locations is due to the fact that the bore conditions are still at their ambient values before projectile arrival. The third curve in each figure plots the conditions at the time of muzzle exit, t3 (1.13 ms).

The rarefaction wave can be seen as a discontinuity in the slope of the fourth and fifth curves. The wavefront is 50 cm from the breech at t4 (1.50 ms) and 10 cm from the breech at t5 (2.28 ms). Finally, the sixth curve shows how the temperature and heat transfer coefficient have continued to decay at t6 (4 ms).

Since the thermal gradient is small in the barrel wall in the axial direction, the gas conditions are evaluated as functions of time at the midpoint of each discrete region of the barrel. As an example, the values of *h* and *T* are plotted in Figure 3 as functions of time for the axial position of 15.2 cm from the breech. As before, the vertical line at 0.67 ms is due to the fact the bore conditions are still in their ambient cool state until the projectile arrives. In this figure, the small rise in the heat transfer coefficient just after 2 ms indicates the arrival of the rarefaction wavefront at that axial position.

For this analysis, the M60 barrel assembly bore surface was divided into eleven regions, shown in Figure 4, for application of the bore wall boundary condition. Logarithmic spacing was used for the calculation points in order to generate smaller regions near the breech where the bore gas properties are more dependent on axial position.

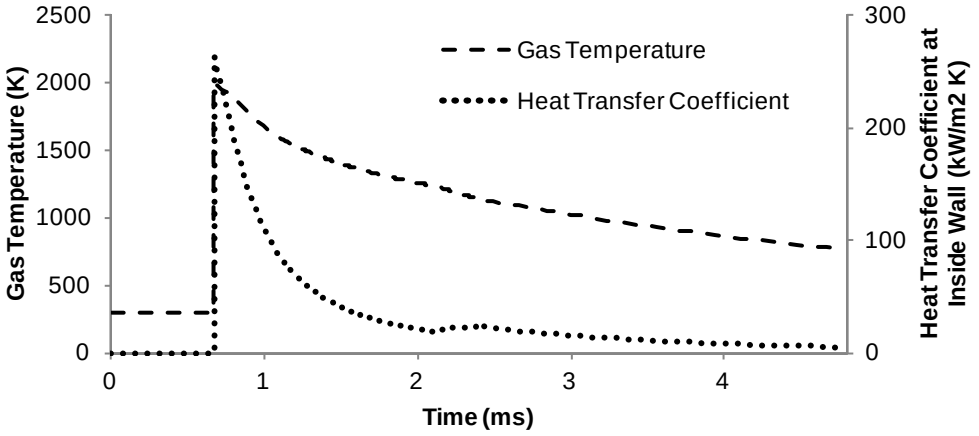

Figure 3. Gas temperature and interior wall heat transfer coefficient vs. time for the axial position of 15.2 cm from the origin of rifling.

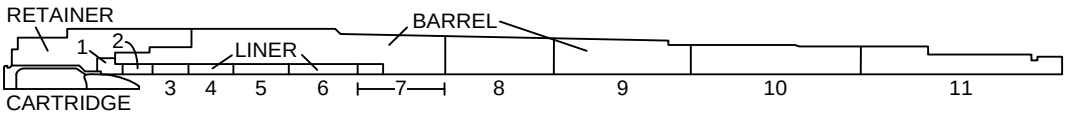

Figure 4. M60 barrel geometry showing discretized regions on the bore surface where a distinct bore boundary condition is applied (not to scale).

Finite Element Model

A two-dimensional axisymmetric representation of the M60 barrel assembly was utilized for the finite element model. The bore wall boundary condition was applied to the eleven regions shown in Figure 4. In order to capture the extremely rapid rise in heat transfer coefficient and gas temperature generated when the projectile passes a given location in the barrel (see Figure 3), a time step of 0.05 milliseconds was utilized in the simulation during the burst firing. Based on this time step, a mesh dependency study was performed to determine the element size required on the bore wall to accurately capture the rapid heat flux as each round is fired. In this model, an element edge size of 0.025 millimeters was utilized along the entire bore surface. The element edge length was permitted to increase by 20% per element in the radial direction with the maximum edge length limited to 5 millimeters for any element in the model.

The convective heat transfer coefficient on the outer surface of the barrel was set to 20 W/m^2-K and an ambient temperature of 298 kelvin was used for both convection and radiation from the outer surface.

The M60 machine gun features a 56-cm long barrel made of 4100 series steel and a Stellite liner which encompasses the first 15 cm of projectile travel. Due to the large temperature range encountered by these materials during the course of an extended burst firing, the model incorporates the temperature-dependent thermal properties of 4130 steel [10] and Stellite 21 [11].

The finite element calculations were performed using the Autodesk® Simulation CFD 2012 software package.

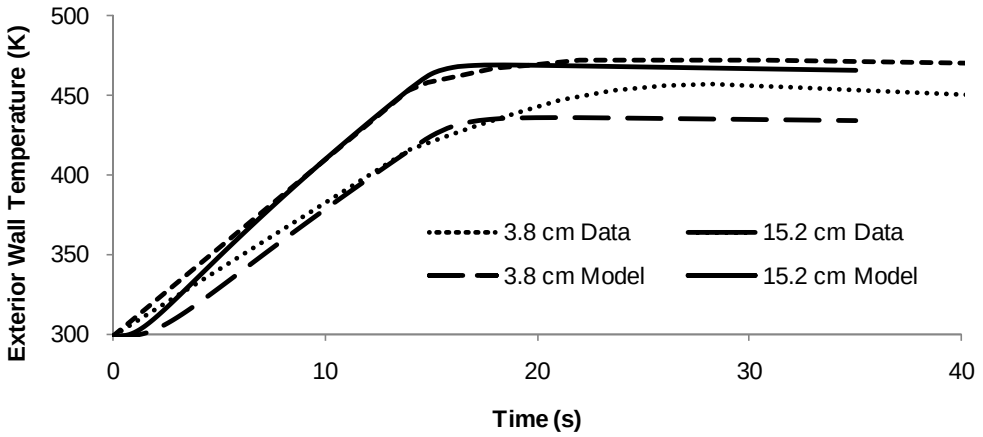

Figure 5. Comparison of model predictions with test data for exterior wall temperature vs. time for two axial positions located at 3.8 cm and 15.2 cm from the origin of rifling.

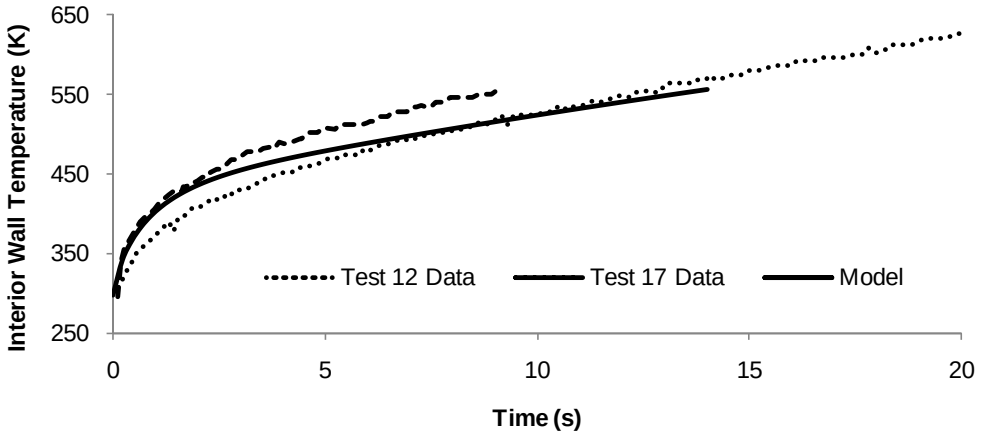

Figure 6. Comparison of model predictions with test data for the interior wall temperature vs. time at 3.8 cm from the origin of rifling.

Comparison with Experimental Data

The results of this analysis are compared with recorded temperature data taken from [12]. In order to properly simulate the test conditions of [12], the firing rate in the model was set to 536 rounds per minute.

Figure 5 presents the outside wall temperature for a 125-round burst at two axial positions – 3.8 cm and 15.2 cm from the origin of rifling. The ambient temperature used in the example simulation is 298 K, which is the same as that of the actual test. There is excellent agreement between the model and the test data for the 15.2 cm position, while the peak temperature at the 3.8 cm position is under predicted by 21 K. Due to the proximity of this measurement location to the breech, it is likely that this discrepancy can be explained by inaccuracy of the K_e factor which attempts to account for the fact that the flow conditions are not fully developed in this region.

Figure 6 plots the predicted inside wall temperature during the same 125-round burst at the axial position of 3.8 cm from the origin of rifling. The simulation results are plotted against the data obtained from Tests 12 and 17 in [12]. The ambient temperatures for these measurements are different than the simulation; Test 12 was conducted when the ambient temperature was 278 K and for Test 17 the ambient temperature was 294 K. Also, Test 12 was a 200 round burst and Test 17 was a 300 round burst, however, the data for Test 17 is truncated at 80 rounds due to a data acquisition anomaly at that point during the test. Due to the similar initial temperatures, the model predictions can be more readily compared to the Test 17 results. Overall, the model agreement with the test data is reasonable. The model initially matches the Test 17 data quite well, but then under predicts the bore surface temperature further into the burst firing. After 80 rounds, the model predicted bore surface temperature is 36 K

below the measured data. This under prediction at the 3.8 cm axial position is consistent with the results on the outer surface of the barrel. Again, the discrepancy can likely be attributed to the K_e factor.

Conclusion

A simplified thermal model has been developed to predict the temperature evolution in machine gun barrels during extended burst firing using a combination of a lumped-parameter interior ballistics calculation and heat conduction in the barrel assembly. Comparison of the model with the limited data available in the open literature provides confidence in the model predictions. One area which warrants further refinement is the entrance factor which modifies the heat flux on the bore wall near the breech to account for the fact that the flow is not fully developed in this region.

While the results presented in this manuscript are limited in scope, the model is easily extended to gain insight into other thermal phenomena such as conduction through the breech into a chambered round to simulate a cook-off event.

References

1. Hill, R.D. and J.M. Conner. 2012. “Transient Heat Transfer Model of Machine Gun Barrels.” *Mater. Manuf. Processes*, 27(8): 840-845.
2. Baer, P.G. and J.M. Frankle. 1962. “The Simulation of Interior Ballistic Performance of Guns by Digital Computer Program,” Report No. 1183, Ballistic Research Laboratories.
3. PRODAS V3 Technical Manual. unpublished, included with PRODAS software from Arrow Tech Associates.
4. Dittus, F.W. and L.M.K. Boelter. 1930. “Heat Transfer in Automobile Radiators of the Tubular Type,” in *University of California Publications in Engineering*, Vol. 2, No. 13, pp. 443-461.
5. Heiney, O.K. 1979. “Ballistics Applied to Rapid-Fire Guns,” in *Interior Ballistics of Guns*, H. Krier and M. Summerfield, eds. Progress in Astronautics and Aeronautics, Vol. 66, American Institute of Astronautics and Aeronautics, pp. 87-112.
6. Heiney, O.K. 1971. “Theoretical Gun Propellant Thermochemical Evaluation,” Technical Report AFATL-TR-71-11, Air Force Armament Laboratory.
7. Kubota, N. 2007. *Propellants and Explosives*, Second Edition, Wiley-VCH GmBH & Co. KGaA, Weinheim, pp. 91-94.
8. Corner, J. 1950. *Theory of the Interior Ballistics of Guns*. John Wiley & Sons, Inc., New York, pp. 364-383.
9. Gerber, N. and M. Bundy. 1991. “Heating of a Tank Gun Barrel: Numerical Study,” AD-A241 136. Memorandum Report BRL-MR-3932. Ballistic Research Laboratory.
10. Hoyt, S.L. (Ed.). 1954. *ASME Handbook, Metals Properties*. McGraw Hill Book Company, Inc. New York.
11. Summary Technical Report of Division 1, NDRC. 1946. *Hypervelocity Guns and the Control of Gun Erosion*, Volume 1.
12. Moeller, C.E. and A.J. Bossert 1973. “Measurement of Transient Bore-Surface Temperatures in 7.62 mm Gun Tubes,” AD-780 938. Midwest Research Institute.

About NTS

National Technical Systems (NTS) provides test, inspection and certification services to help clients build better, stronger, safer, more reliable products and bring those products to market quickly and efficiently. Our capabilities span a very wide spectrum, covering environmental, dynamics, EMC, wireless, product safety, materials, ballistics and more. NTS engineers and technicians have extensive knowledge of current test and conformity requirements, both domestic and international over a range of industries including aerospace, defense, telecom and energy.

NTS
24007 Ventura Blvd.
Suite 200
Calabasas, CA 91302

www.nts.com | 1.800.270.2516 | sales@nts.com